Supplement of Eur. J. Mineral., 36, 1023–1036, 2024
https://doi.org/10.5194/ejm-36-1023-2024-supplement

European Journal of Mineralogy
Open Access

Supplement of

The coesite–stishovite transition of hydrous, Al-bearing SiO_2: an in situ synchrotron X-ray study

Monika Koch-Müller et al.
Correspondence to: Monika Koch-Müller (monika.koch-mueller@gfz-potsdam.de)

Supplement

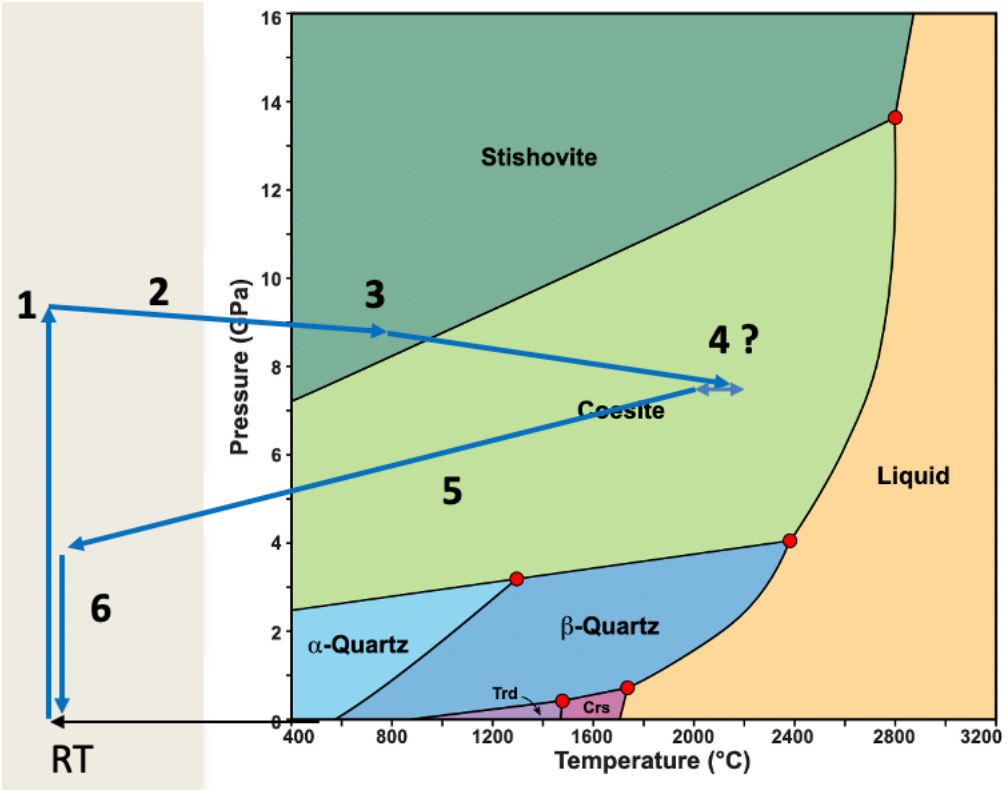

Figure S1. Modified *P-T* diagram of the system SiO_2 after John Brady (copy right) (https://www.science.smith.edu/~jbrady/petrology/petrology-topics/assem/assem-figure03.php) showing exemplarily the experimental approach. See manuscript for more information on the *P-T* paths and points (1-6) of the experiments.

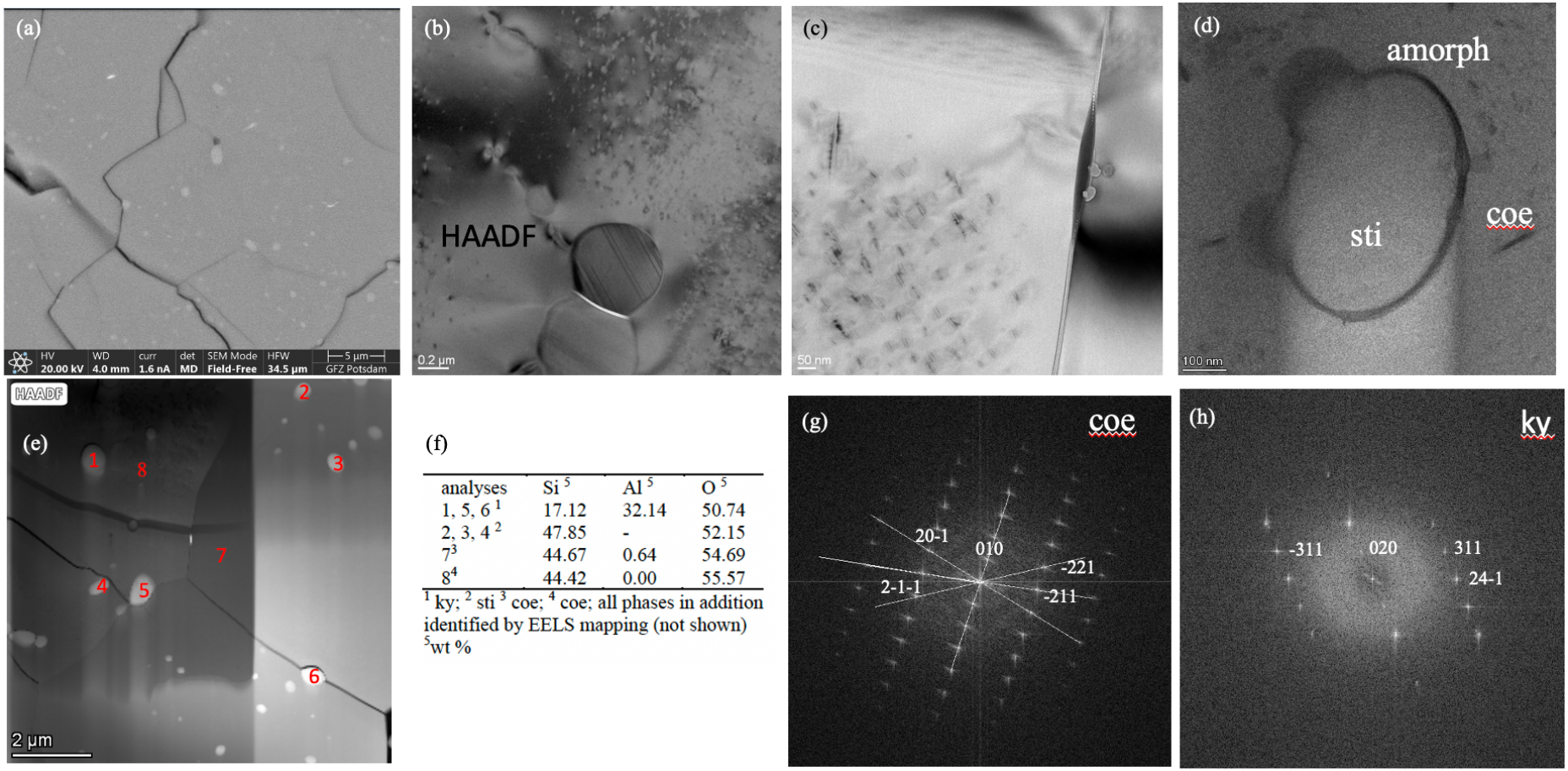

analyses	Si [5]	Al [5]	O [5]
1, 5, 6 [1]	17.12	32.14	50.74
2, 3, 4 [2]	47.85	-	52.15
7 [3]	44.67	0.64	54.69
8 [4]	44.42	0.00	55.57

[1] ky; [2] sti [3] coe; [4] coe; all phases in addition identified by EELS mapping (not shown)
[5] wt %

Figure S2. (a) Representative SE image of a part of sample BT-745; the light round to elongated spots turned out to be Ky and Sti; (b), (c) BF images showing nm-sized round and elongated Ky and Sti inclusions; (d) Sti inclusion with an amorphous SiO_2 rim within Coe; (e) location of some energy dispersive spectra of the inclusions in Coe; (f) results of the energy dispersive spectra of the points shown in (e); (g) and (h) indexed electron diffraction pattern for Coe and Ky, respectively. Crystal structure data for Coe and Ky from Smyth et al. (1987) and Yang et al. (1997), respectively.

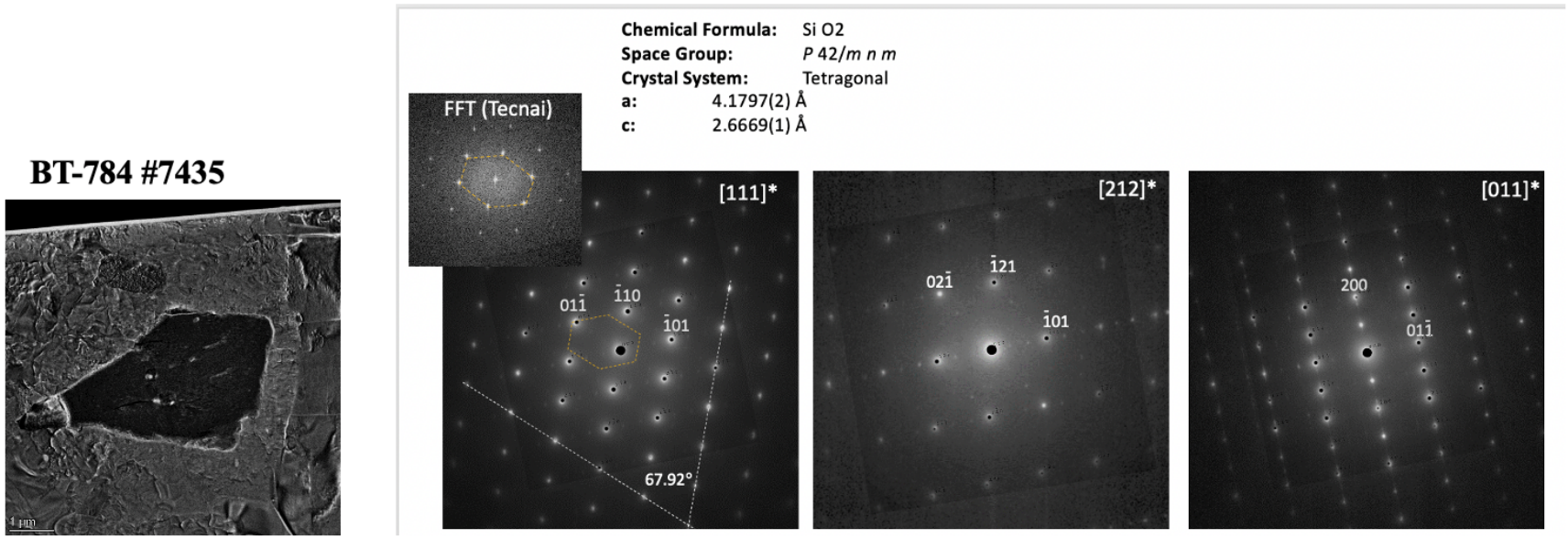

Figure S3. BF image of a part of the FIB foil of sample BT-784 with a Sti crystal in Coe matrix (left) and corresponding electron diffraction pattern (right). Notice superstructure spots in all diffraction pattern. Crystal structure data for Sti from Sugiyama et al. (1987).

Electron Energy Loss Spectroscopy (EELS) and EELS Mapping

For further analyses we have cut FIB foils through Stis and Coe grains of sample BT-783 and BT-784 and characterized the phases by high resolution electron diffraction, energy dispersive and electron energy loss spectroscopy. The parts of the foils and the corresponding electron energy loss spectra of Sti, Coe and Ky are shown in Fig. S4. We cannot go into details of the method for the EEL spectroscopy but important to know is, that EELS is sensitive to the local atomic coordination as well as to the electronic structure. One can clearly see in Fig. S4 that the Coe, Sti, and Ky have distinct spectra and they can with the help of these spectra be distinguished in the FIB foil by EELS mapping. Compared to electron diffraction, this is an equally precise but comparatively, very quick method for phase identification (Roddatis et al., 2024). We applied the EELS catalogue and performed EELS mapping to visualize the occurrence of Coe, Sti and Ky in the FIB foils of sample BT-783, BT-784 and BT-745. Results of the EELS mapping for sample BT-784 and BT-783 are shown in Fig. 5 a. and 5 b. With this method we could identified the matrix in Fig. 5 a as Coe and the darker crystals as Sti. In Fig. 5 b. the matrix could be identified as Coe and the worm-like features as Sti but in addition, the round and elongated features were identified as Ky.

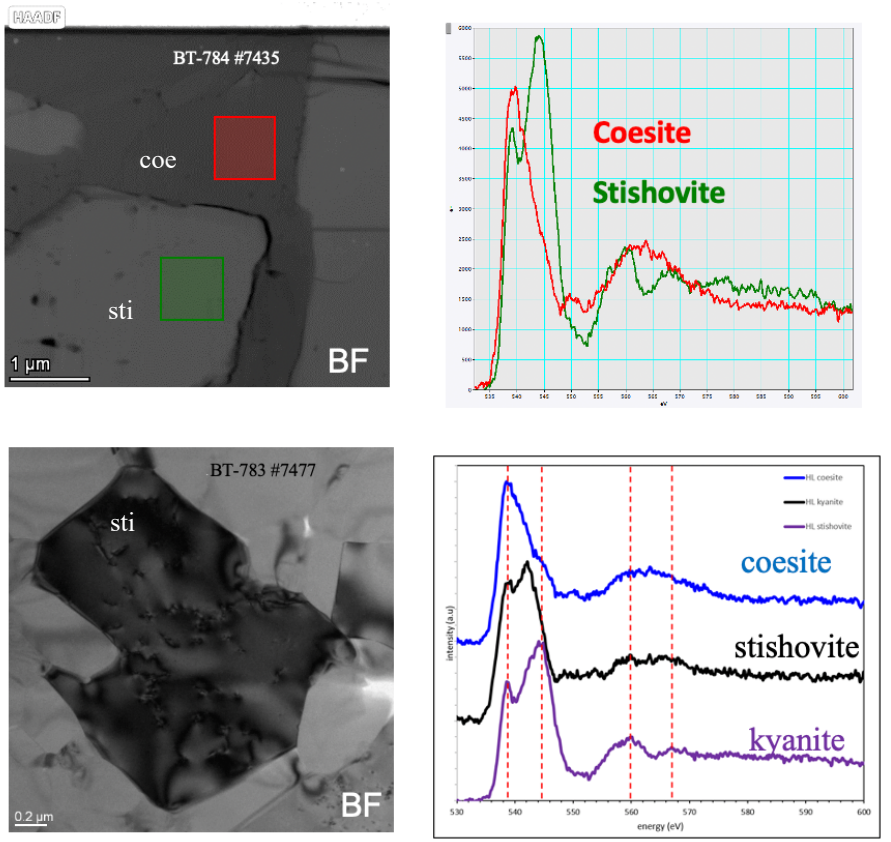

Figure S4. upper part: (left) part of the FIB foil for sample BT-784 and location and raster size for the EELS measurement; (right) EEL spectra; lower part: (left) part of the FIB foil for sample BT-783, where the EEL spectra on the right side were taken. Sti and Coe in both samples were identified by HREM, e.g. Fig S3.

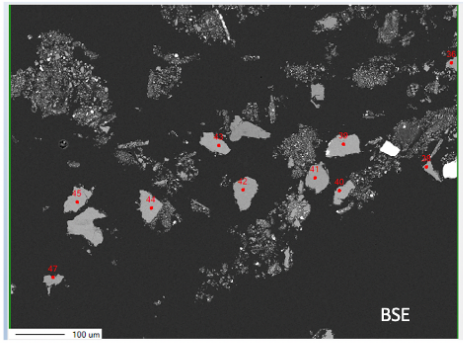

Compositions of selected sti and coe by EPMA

pt	polymorph	SiO_2 WDS	Al_2O_3 WDS	sum
39	coe	98.83	0.50	99.33
40	coe	98.39	0.97	99.36
41	sti	98.07	0.96	99.03
42	sti	98.28	1.23	99.51
43	coe	99.24	0.61	99.85
44	coe	98.85	0.81	99.66
18	*sti*	*98.59*	*1.70*	*100.29*
28	*coe*	*97.51*	*1.67*	*99.18*
30	*coe*	*96.52*	*3.83*	*100.35*

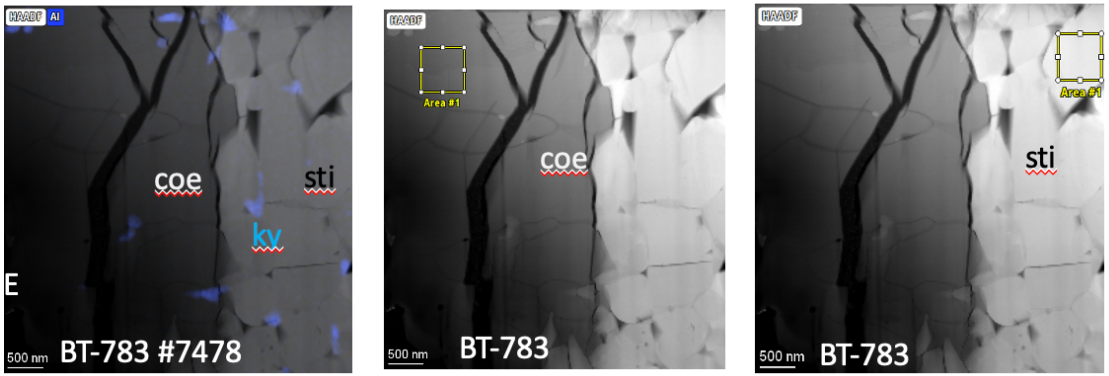

Figure S5. Upper left: BSE image of a part of the sample mount BT-783 showing some of the polished grains (pt labeled 39 - 44), which were identified by Raman spectroscopy as Coe or Sti; upper right: corresponding EPM analyses of the grains 39 – 44, with realistic Al-contents; grain 18, 28, 30 (not shown here) are representative examples of EPA analyses falsified by the nm-sized Ky inclusions.
Lower column: Part of a FIB foil of sample BT-783 with coexisting Coe and Sti (HREM); left: showing in addition in blue the occurrence of Ky inclusions based on EDS Al-mapping; middle and right: showing a representative size and location for the measurements of the energy dispersive spectra in Coe and Sti, respectively, under avoidance of contributions from Ky. Average analyses of 4 measurements yielded 0.90 wt % Al_2O_3 and 99.10 wt % SiO_2 for Coe and 1.28 wt % Al_2O_3 and 90.72 wt % SiO_2 for Sti.

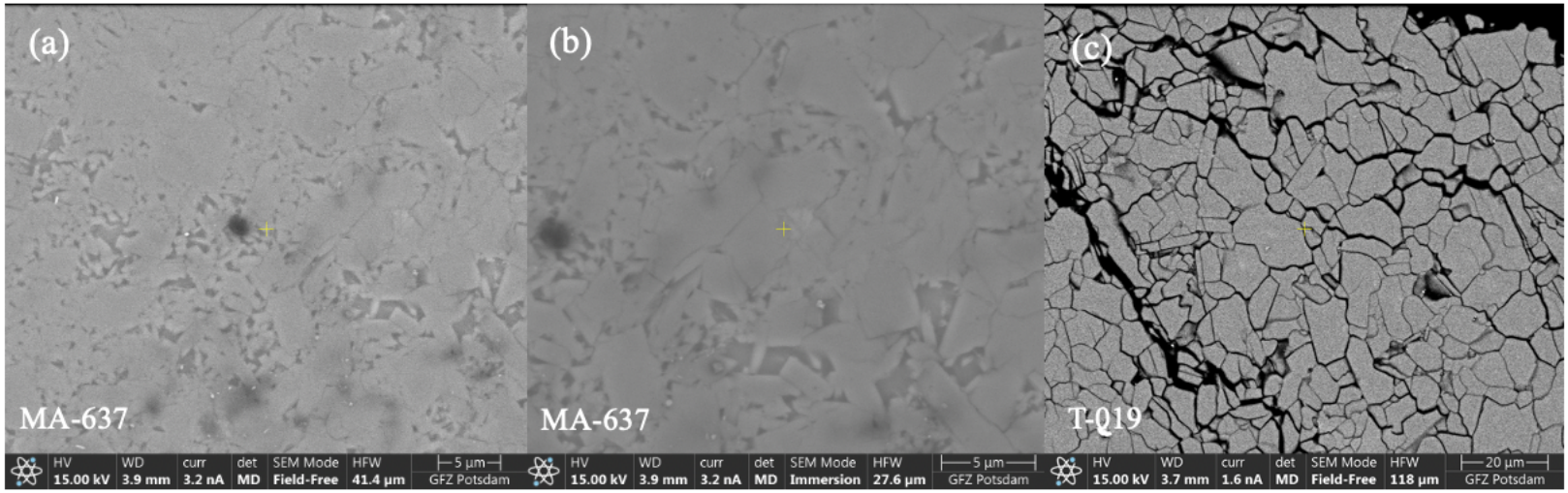

Figure S6. BSE images of parts of the sample mounts of the quench experiments MA-637 and T-019.

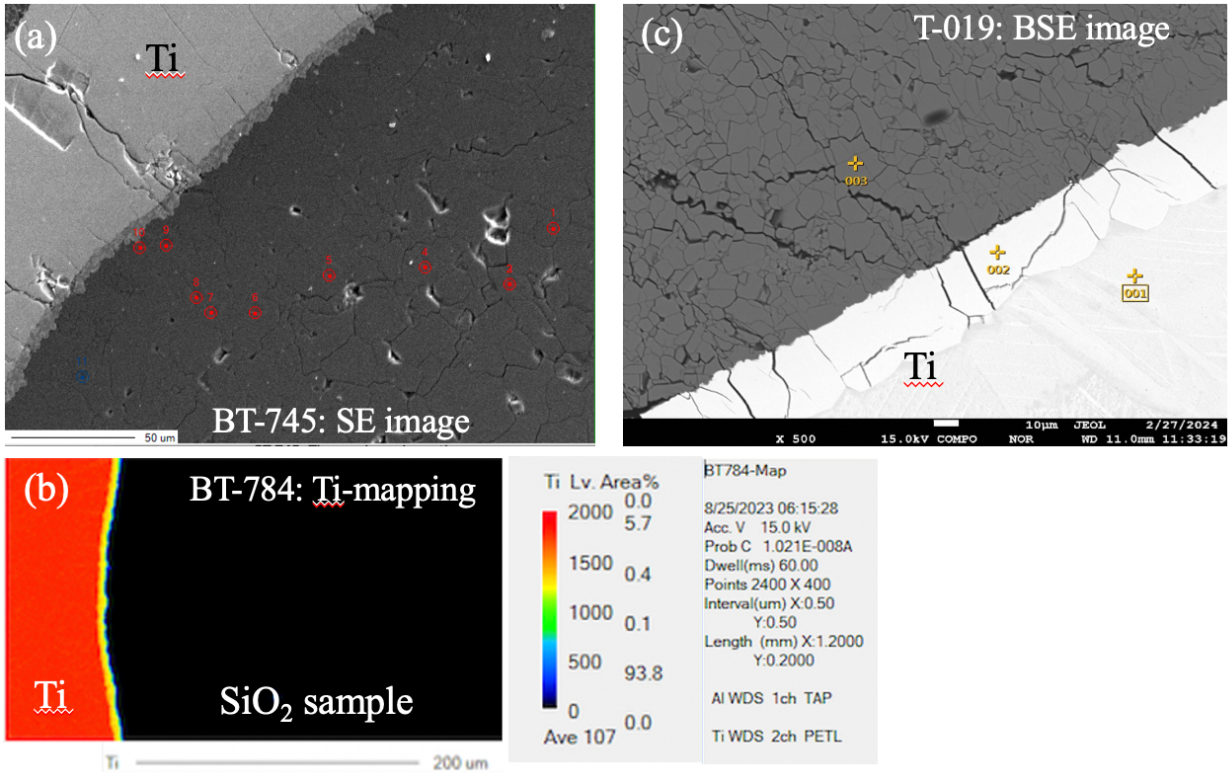

Figure S7. Images from the EPM: (a) SE image of a part of the polished sample mount of BT-745 with part of the Ti-capsule wall (light grey) and SiO_2 sample (black) attached, indicating a reaction rim between Ti and the SiO_2 sample; red points indicate spots for EPM-analyses - there is no detectable Ti in the SiO_2 sample; according to energy dispersive spectra, the reaction rim consists of 75 wt % Ti and 25 wt % Si, which corresponds to a Ti_5Si_3 compound. (b) Ti-mapping of a part of the sample (BT-784) including the Ti-wall of the capsule (red) and showing the reaction rim (yellow); there is no detectable Ti in the SiO_2 sample; (c) BSE image of a part of the polished sample mount of T-019 without reaction rim between Ti and SiO_2. See text for more details.

Table S1. Experimental details and results of the in situ experiments at DESY.

Run	sti synthesis *P*, *T*, time (GPa, °C, min)	Total Nr. of ED XRD of sample	Total Nr. of ED XRD MgO	Total time (min) from synthesis until quench	*P*, *T*, Sti:Coe ratio (GPa, °C) before *T*-quench[1]	Phases in the recovered sample and methods used for characterization
BT-745	8.0, 800, 30[2]	44	19	165	8, 1300, 1:4	Coe (R, TEM), Ky (TEM)
BT-782	8.3, 900, 36	29	16	230	6.8, 1250, 1:1	Coe (R), Sti (R)
BT-783	9.0, 1000, 42	22	17	204	8.4, 1450, 1:1	Coe (R, TEM), Sti (R, TEM), Ky (TEM), Sti:Coe 1:2.5 (XRPD)
BT-784	8.4, 1000, 28[2]	29	10	205	7.7, 1275, 1:1	Coe (R, TEM), Sti (R, TEM), Ky (TEM)
BT-785	8.8, 800, 32[2]	30	17	239	8.5, 1100, 2:3	Coe (R), Sti (R)
BT-786	8.0, 700, 36[2]	41	12	225	7.4, 1075, 2:3	Coe (R), Sti (R)

[1] the same ratio was always observed after quenching (when determined)
[2] in addition to Sti metastable Coe was formed during *T* increase below 1000 °C but vanished at higher *T* during the performance of the experiments
Abbreviations: R: Raman spectroscopy, TEM: transmission electron microscopy, XRPD X-ray powder diffraction

Table S2. Results of X-ray powder diffraction analyses using the Rietveld method of solid run products of selected experiments.
Cell-dimensions of stishovite and coesite from literature are given for comparison.

Run #	products (wt %)	*a*(Å)	*b*(Å)	*c*(Å)	*ß*(°)	*V*(Å^3)
MA-637	Coe (8)	7.14(2)	12.38(2)	7.18(2)	120.4(1)	547.2(9)
	Sti (92)	4.1822(5)		2.6681(3)	90.0	46.67(1)
T-016	Coe (100)	7.1376(8)	12.373(1)	7.1753(6)	120.33(2)	546.89(9)
T-019	Coe (100)	7.139(3)	12.380(4)	7.174(2)	120.32(2)	547.3(2)
BT-783	Coe (70)	7.133(7)	12.37(1)	7.176(5)	120.33(4)	546.6(6)
	Sti (30)	4.178(1)		2.666(1)	90.0	46.54(5)
literature	Sti*	4.179		2.665	90.0	45.81
	Coe**	7.1367	12.3695	7.1742	120.337	546.6

*Kroll and Milko (2003)
**Geisinger et al. (1987)

References:

Brady, J.: (https://www.science.smith.edu/~jbrady/petrology/petrology-topics/assem/assem-figure03.php)

Geisinger, K. L., Spackman, M. A., and Gibbs, G. V.: Exploring of structure, electron density distribution, and bonding in coesite with Fourier and pseudo atom refinement methods using single-crystal X-ray diffraction data, J. Phys. Chem., 91, 3237-3244, 1987.

Kroll, P., and Milko, M.: Theoretical investigation of the solid-state reaction of silicon nitride and silicon dioxid forming silicon oxynitride (Si_2N_2O) under pressure, Z. Anorg. Allg. Chem., 629, 1737-1750, https://doi.org/10.1002/zaac.2003300122, 2003.

Roddatis, V., Kovaleva, E., Syczewski, M., Schreiber, A., Wirth, R., Koch-Müller M.: Electron energy loss spectroscopy for differentiating of minerals polymorphs. BIO Web of Conferences 129, 06032 EMC 2024, Https://doi.org/10.1051/bioconf/202412906032, 2024.

Smyth, J. R., Smith, J. V., Artioli, G., and Kvick Å.: Crystal structure of coesite, a High-Pressure form of SiO_2, at 15 and 298 K from Single-Crystal Neutron and X-ray Diffraction Data: Test of Bonding Models, J. Phys. Chem., 91, 988-992, 1987.

Sugiyama, M., Endo, S., Koto, K.: The crystal structure of stishovite under pressure up to 6 GPa: sample at 1 bar, Mineral. Jour., 13, 455-466, 1987.

Yang, H., Downs, R. T., Finger, L. W., Hazen, R. M., and Prewitt, C. T.: Compressibility and crystal structure of kyanite, Al_2SiO_5, at high pressure, Am. Mineral., 82, 467-474, 1997.